

DICE: Disentangling Artist Style from Content via Contrastive Subspace Decomposition in Diffusion Models

Tong Zhang¹, Ru Zhang^{1,*}, Jianyi Liu¹,

¹ Beijing University of Posts and Telecommunications, School of Cyberspace Security, Beijing, 100876,

*Corresponding author

Abstract

The recent proliferation of diffusion models has made style mimicry effortless, enabling users to imitate unique artistic styles without authorization. In deployed platforms, this raises copyright and intellectual-property risks and calls for reliable protection. However, existing countermeasures either require costly weight editing as new styles emerge or rely on an explicitly specified editing style, limiting their practicality for deployment-side safety. To address this challenge, we propose DICE (Disentanglement of artist Style from Content via Contrastive Subspace Decomposition), a training-free framework for on-the-fly artist style erasure. Unlike style editing that require an explicitly specified replacement style, DICE performs style purification, removing the artist's characteristics while preserving the user-intended content. Our core insight is that a model cannot truly comprehend the artist style from a single text or image alone. Consequently, we abandon the traditional paradigm of identifying style from isolated samples. Instead, we construct contrastive triplets to compel the model to distinguish between style and non-style features in the latent space. By formalizing this disentanglement process as a solvable generalized eigenvalue problem, we achieve precise identification of the style subspace. Furthermore, we introduce an Adaptive Attention Decoupling Editing strategy dynamically assesses the style concentration of each token and performs differential suppression and content enhancement on the QKV vectors. Extensive experiments demonstrate that DICE achieves a superior balance between the thoroughness of style erasure and the preservation of content integrity. DICE introduces an additional overhead of only 3 seconds to disentangle style, providing a practical and efficient technique for curbing style mimicry.

1. Introduction

In recent years, diffusion models have demonstrated remarkable capabilities in fields such as artistic creation, generating exceptional works of art from textual descriptions and reference images. This creative ability stems from their training on vast amounts of data, including artist styles and artworks, but it has also given rise to severe copyright and ethical challenges. The problem of style mimicry is particularly acute, where users can maliciously replicate a specific artist's style on a large scale simply by using prompts such as {in the style of [target style]} without authorization. This practice not only undermines the uniqueness and market value of an artist's work but also constitutes a direct infringement of their intellectual property rights, posing a significant threat to the creative arts field. The question of how to provide model deployers and platforms with efficient method to erase specific artistic styles, thereby protecting intellectual property while preserving the model's general utility has become a pressing issue in the field of controllable Artificial Intelligence.

Research on mitigating related risks includes concepts erasure, style transfer, and data perturbation [35], etc. Concepts erasure refers to preventing the model from generating images containing specific concepts. Current research can be divided into fine-tuning [4, 12, 25, 54], weight-editing based on optimization [6, 23, 27, 43], and inference-time intervention. Fine-tuning [24, 29] refers to retraining or fine-tuning the model. Weight-editing based on optimization, such as closed-form solution editing [13, 44], analytically derives weight updates from a loss function to avoid iterative retraining. Inference-time intervention refers to editing the internal features of the model during inference. Technically, methods for separating and controlling styles also include style transfer, which involves replacing the style of one image with another while retaining the content and structure.

These methods have limitations in resisting style mimicry: Starting from the time and operational costs in practical applications, either they are constrained by the

high cost of weight editing, which requires re-adjusting the model for each newly added artist style. These style editing methods are essentially style expression/style substitution. They require explicitly specifying the style to be replaced, which turns into "selecting a replacement style for the user" rather than "preventing the generation of a certain style", and is restricted when dealing with large-scale styles. Mapping the target to an null text or a neutral style often leads to image distortion or a reduction generation diversity. In terms of erasing effect, these methods that rely on textual guidance cannot achieve complete style erasure and content preservation. Instead, they often achieve style erasure at the cost of damaging the overall image structure, core content, and aesthetic quality. We posit that the root of this deficiency lies in these methods conceptually equating style with a concrete object. An artist's style is a diffuse, abstract concept that permeates the model's entire representational distribution [53]. Subjecting it to conventional erasure inevitably damages the entangled content structure, forcing a trade-off where style removal is achieved only at the cost of sacrificing content integrity.

This exposes a fundamental flaw in existing techniques: they compel the model to erase a concept it does not truly comprehend. We argue that a model cannot discern what constitutes style from a single text or image alone [41, 42]. To enable the model to precisely understand the "style" to be erased and the "content" to be preserved, we depart from the conventional single-prompt paradigm. Instead, leveraging the malicious user's prompt, we construct a triplet sample {Anchor, Positive, Negative} centered on the target artist's style. This triplet comprises: an image with the target style and content, an image with the target style but different content, and an image with different style but the same content. This framework allows the model to learn the distinct features of style and content by contrasting the differences among these images.

Furthermore, we formalize the problem of disentangling style and content within the latent space as a solvable generalized eigenvalue problem. Based on this, we propose DICE (Disentanglement of artist Style from Content via Contrastive Subspace Decomposition), a training-free framework for on-the-fly artist style erasure. Unlike other methods that require specifying the replacement style, DICE achieves a purifying erasure of the artist's features, achieving a balance between style erasure and content preservation. By maximizing the stylistic commonality between the anchor and positive samples while minimizing the content similarity between the anchor and negative samples, DICE formulates the style-content disentanglement task as a solvable optimization problem. This allows for the derivation of a subspace that captures the core style features during inference. We also introduce an attention decoupling editing strategy. Observing that the Query, Key, and Value vec-

tors in the attention mechanism govern different aspects of the generated output, we apply orthogonal suppression to the style and texture-related K and V vectors, while simultaneously applying content-enhancement guidance to the structure-related Q vector to mitigate content loss. Finally, to address the varying intensity of artistic style across different image patches, we propose an Adaptive Erasure Controller. This component dynamically calculates the style concentration for each token and allocates a corresponding erasure strength via a soft-thresholding function, enabling precise and efficient style removal. This provides a practical and robust technical solution to curb style mimicry. In summary, our contributions are as follows:

- We propose DICE, a novel artist style erasure framework designed to combat style mimicry. Operating at inference-time directly from a malicious user's prompt, it provides a practical and efficient solution for deployment-side style purification without requiring an explicitly specified replacement style or per-style model updates.
- By constructing contrastive triplets, we formalize the problem of style and content disentanglement in the latent space as a solvable generalized eigenvalue problem.
- We introduce the Attention Decoupling Editing strategy and the Adaptive Erasure Controller, which perform adaptive and differentiated editing on the Q, K, and V matrices of the self-attention module to achieve precise style erasure and content preservation.
- Extensive experiments conducted on multiple artist styles demonstrate that our method achieves the optimal balance between the thoroughness of style erasure and the integrity of content preservation.

2. Related Work

2.1. Concept erasure

Current concept erasure methods for diffusion models are primarily divided into three categories: fine-tuning, weight-editing based on optimization, and inference-time interventions.

Fine-tuning. Fine tuning achieves concept erasure by training on additional datasets or with extra lightweight modules and learnable vectors. Representative works such as SPM [28] and CFG guidance [11] are realized by training learnable vectors for specific concepts [28], training lightweight erasure modules [19], improving classifier guidance [18], adversarial training [20], knowledge distillation [21], and continual learning [15]. EraseDiff [47] guides the model to deviate from paths related to the concept being erased during the generation process, while designing a balanced objective to minimize the impact on other concepts, thereby achieving a balance between concept erasure and generation quality. SuMA [30] learns a linear projection to map the model's representation space to a specific subspace,

in which the target concept’s representation is completely removed. This approach, while erasing the concept, can better preserve the integrity of other content. Although these algorithms are effective, the required computation time and inference costs are high, and most methods struggle to handle newly added erasure concepts in real-time, as they require retraining.

Weight-editing based on optimization methods are represented by closed-form solution editing[23, 24]. Closed-form solution editing directly solves for model weight updates by deriving from the loss function, avoiding the computational overhead of iterative optimization and significantly improving editing efficiency. Chen et al. [6] proposed the concept of Growth Inhibitors, which suppress the expression of inappropriate concepts by re-weighting specific features during the diffusion sampling process, without modifying the model. Furthermore, Ahmed et al. [1] proposed a source-free machine unlearning framework that directly modifies model parameters by applying approximate calculations and closed-form updates, thereby removing the influence of specific information without accessing the original dataset. Furthermore, Neuron-level intervention methods control concept generation by locating and suppressing the activation of specific neurons. As represented by studies [49] and [5], this is achieved by locating neurons sensitive to concept editing, pruning key neurons via masking, and reducing the sensitivity of concept-editing-related neurons.

inference-time interventions. Inference-time interventions refer to the editing of internal features of the model during the inference process, such as attention maps or activations. Xiong et al. [48] introduced a zero-shot framework for concept erasure through dynamic text embedding neutralization via co-occurrence encoding, calibrated vector subtraction, and visual feedback loops. liu et al. [26] innovates with prompt embedding redirection to route unsafe semantics away from harmful regions, ensuring persistence against adversarial attacks. IRECE [46] enhances robustness by localizing concepts via cross-attention analysis and perturbing associated latents during denoising. Furthermore, GLoCE [22] introduces a gated low-rank adaptation module that selectively activates for target concepts, enabling precise localized erasure in mixed-prompt scenarios without any training.

Content Preservation. Research on preserving non-target concepts includes methods like modifying anchors [53], loss control [23], and subspace mapping [30]. SLECT [53] proposed a dynamic anchor selection framework based on causal tracing and "Sibling-Exclusive Concepts" (SECs) to achieve precise erasure of target concepts while better preserving contextual semantics. SPEED [23] introduced a scalable model editing framework that utilizes an Influence-based Prior Filter (IPF) and Invariant Equality

Constraints (IEC) to efficiently erase a large number of concepts while proactively preserving the semantic integrity of non-target concepts.

2.2. Style Transfer

Style transfer is a technique that modifies the artistic style of an image while aiming to preserve its core content. Hertz et al. [16] proposed to connect text tokens and spatial regions through cross-attention, precisely re-weight or replace the cross-attention graph to achieve style rendering. He et al. [14] proposed that certain layers and activations in the pre-trained diffusion model correspond to style information. They achieved the decoupling of artistic styles by selectively combining the contents and activation values from different layers. Fahim et al. [9] preserves content through dual-path attention aggregation and enhances style injection via attention component modulation, applicable to both image and prompt driven scenarios. Zhang et al. [52] modulates intermediate diffusion samples with the Fourier phase spectrum of the content image to guide stylization while retaining edge structures and integrating homomorphic semantic features for improved preservation. These methods are related to the artist style erasure technology, all involving the separation or control of styles within the model. However, these methods usually require explicit specification of alternative approaches. When mapping the style to Null text or a fixed style to prevent style mimicry, it may disrupt the generated content or reduce the diversity of the generation. Therefore, these methods may be limited in their ability to resist style plagiarism.

2.3. Data Perturbation

Data perturbation is another method to deal with style mimicry. It involves making imperceptible changes to the images, ensuring that any malicious users who attempt to exploit these perturbed data to fine-tune the model will ultimately only obtain ineffective style replication results. Glaze [35] proposed a data-level defense method that adds imperceptible style cloaks to artworks before their release, misleading the model into learning an incorrect style, thereby protecting the artist’s original style from being mimicked. Ahn et al. [2] introduce a nearly zero-cost protection mechanism that applies minimal perturbations to render images resistant to personalization in diffusion models. By targeting the fine-tuning process directly, their technique ensures that personalized models fail to capture the intended style, with low computational overhead making it accessible for individual artists. Passananti et al. [31] extended style protection techniques from images to the video domain by extracting a consistent style vector and applying temporally coherent adversarial perturbations to defend against video generation models’ mimicry of dynamic styles. Nightshade [36] introduced a prompt-specific

”data poisoning” attack designed to hide the artist’s style and contaminate the model’s understanding of related concepts, thereby disrupting its ability to generate images in that specific style.

3. Preliminary

3.1. Latent Diffusion Models

Latent Diffusion Models (LDMs) [33] generate high-resolution images by denoising a latent variable in a low-dimensional space. A U-Net-based noise predictor ϵ_θ iteratively transforms random Gaussian noise z_T into a clean latent z_0 by predicting the noise in z_t at each timestep t . Given a text prompt p encoded as $c = T_v(p)$, LDMs adopt Classifier-Free Guidance (CFG) [17], which combines conditional prediction (with c) and unconditional prediction (with a null prompt c_\emptyset) to obtain the final noise estimate $\hat{\epsilon}$ that guides the denoising direction:

$$\hat{\epsilon}(z_t, t, c) = \epsilon_\theta(z_t, t, c_\emptyset) + s \cdot (\epsilon_\theta(z_t, t, c) - \epsilon_\theta(z_t, t, c_\emptyset)) \quad (1)$$

where s is the guidance scale factor. The U-Net consists of residual and self-attention blocks. Self-attention [37] captures long-range dependencies in an intermediate feature map ϕ by first computing Query (Q), Key (K), and Value (V):

$$Q = W_Q(\phi), \quad K = W_K(\phi), \quad V = W_V(\phi) \quad (2)$$

where W_Q, W_K, W_V are learnable linear projection matrices. Subsequently, a weighted sum of V is computed based on the dot-product similarity between Q and K to produce the layer’s output:

$$\text{Attn}(Q, K, V) = \text{softmax}\left(\frac{QK^\top}{\sqrt{d}}\right)V \quad (3)$$

3.2. Canonical Correlation Analysis

Canonical Correlation Analysis (CCA) [45] is a classical multivariate statistical method for analyzing the correlation between two sets of multidimensional variables. Its core objective is to find linear combinations of the two variable sets that maximize the correlation between these new combinations. Given two centered data matrices $X \in \mathbb{R}^{N \times D_1}$ and $Y \in \mathbb{R}^{N \times D_2}$, where N is the number of samples, and D_1 and D_2 are the feature dimensions, CCA seeks to find a pair of projection vectors, $u \in \mathbb{R}^{D_1}$ and $v \in \mathbb{R}^{D_2}$, that maximize the correlation between the new projected variables Xu and Yv . This optimization problem can be formulated as:

$$\underset{u, v}{\text{argmax}} \text{corr}(Xu, Yv) = \frac{u^T \Sigma_{XY} v}{\sqrt{(u^T \Sigma_{XX} u)(v^T \Sigma_{YY} v)}} \quad (4)$$

Here, $\Sigma_{XX} = \frac{1}{N-1} X^T X$ and $\Sigma_{YY} = \frac{1}{N-1} Y^T Y$ are the sample covariance matrices of X and Y , respectively, and

$\Sigma_{XY} = \frac{1}{N-1} X^T Y$ is the sample cross-covariance matrix between X and Y . This maximization problem can be shown to be equivalent to solving a Generalized Eigenvalue Problem [45]:

$$\Sigma_{XY} \Sigma_{YY}^{-1} \Sigma_{XX} u = \rho^2 \Sigma_{XX} u \quad (5)$$

where ρ is the canonical correlation coefficient. It is required that the covariance matrices Σ_{XX} and Σ_{YY} be positive definite, which ensures they are invertible.

4. Method

Our method aims to achieve the precise erasure of artistic style while maximally preserving the image’s content structure. The complete DICE framework comprises two stages: 1) Subspace Capture: By constructing triplets and aligning patches, we formalize the optimization problem of disentangling style and content within the latent space as a generalized eigenvalue problem, which is then solved to obtain the style and content subspaces. 2) Guided Erasure and Preservation: During the image inference and denoising process, these computed style and content subspaces are utilized to perform precise style erasure and ensure content preservation.

4.1. Triplet Contrastive Construction

We posit that existing style erasure methods often damage content because they fail to truly comprehend the abstract concept of ”style” that needs to be erased. The root of this problem is the model’s difficulty in learning what constitutes content versus style from a single text description or a single reference image [7, 39]. In practice, for an abstract concept like artistic style [53], text alone can hardly delineate complex visual characteristics such as brushwork and texture, whereas an image contains far richer information. Consequently, we abandon the traditional paradigm of mining style from a single sample and instead enable the model to learn from a comparison of images. To counter style mimicry, we start from the user’s prompt, such as ”A flower in the style of Van Gogh”, and construct a triplet sample $\{\text{Anchor}, \text{Positive}, \text{Negative}\}$ corresponding to three types:

- **Anchor (P_A)** : Contains the artistic style to be erased and the content to be preserved (”A flower in the style of Van Gogh”).
- **Positive (P_P)** : Contains the artistic style to be erased but with different content (”A road in the style of Van Gogh”).
- **Negative (P_N)** : Contains different artistic styles but the same content to be preserved (”A flower in the style of Monet”).

By constructing this contrastive triplet, we provide the model with a clear frame of reference, enabling it to understand the distinct content and style features we aim to separate (Figure 1). We feed the triplet samples P_A, P_P, P_N

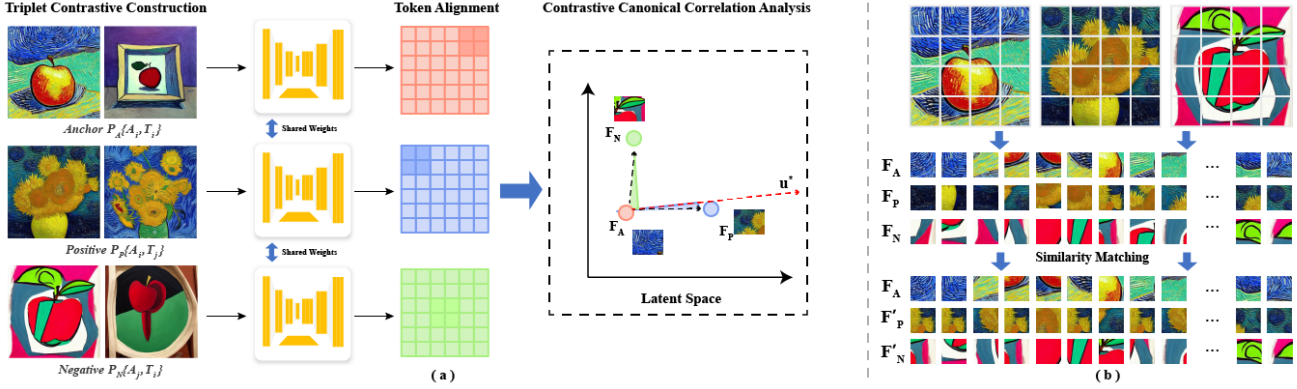


Figure 1. The style subspace identification in DICE. (a) We construct contrastive triplets and feed their features into a Contrastive Canonical Correlation Analysis (CCA), which formalizes style-content disentanglement as a generalized eigenvalue problem to find the style direction u^* . (b) The Token Alignment mechanism corrects spatial misalignment before CCA.

into the pretrained diffusion model and extract their feature maps $F_A, F_P, F_N \in \mathbb{R}^{C \times H \times W}$ from specific diffusion steps and shallow layers [3, 16, 40]. At this stage, the feature maps contain rich semantic information while retaining enough spatial and textural details, which is crucial for accurately disentangling style and content. We then reshape these feature maps into patch matrices $F_A, F_P, F_N \in \mathbb{R}^{N \times D}$, where N is the number of patches and D is the feature dimension of each patch. During the inference process for the triplet samples, even when using the same initial sampling and random seed, minor modifications in the prompts and the inherent stochasticity of the generation model can lead to spatial misalignments (e.g., in position or size) of the content across the three samples. For instance, naively comparing a background patch from the Anchor with a central content patch from the Negative could introduce content noise, preventing the model from correctly identifying the style through a rational comparison. Therefore, we perform a semantic alignment on the feature triplets F_A, F_P, F_N . We compute the cosine similarity [38] between pairs of feature patches to measure their directional proximity in the latent space. Using the Anchor F_A as a reference, we find the most semantically matching patches in F_P and F_N . First, we compute the cosine similarity between all patch pairs of F_A and F_P , yielding a similarity matrix S_{AP} :

$$S_{AP}[i, j] = \frac{F_A[i] \cdot F_P[j]}{\|F_A[i]\| \|F_P[j]\|} \quad (6)$$

where $F_A[i]$ is the i -th patch feature vector of F_A . For each row i of S_{AP} , we find the column index j^* that has the maximum value, indicating that the j^* -th patch of the Positive sample is the most similar to the i -th patch of the Anchor. Based on these indices, we index patches in F_P to form F'_P :

$$F'_P[i] = F_P[j^*] \quad \forall i \in [1, N] \quad (7)$$

By performing the same operation with F_N , we obtain a semantically aligned triplet $F_A, F'_P, F'_N \in \mathbb{R}^{N \times D}$. This is intended to prioritize anchor-driven semantic consistency and avoid injecting content noise under spatial misalignment.

4.2. Contrastive Canonical Correlation Analysis

Given the patch-aligned triplet samples F_A, F'_P, F'_N , our objective is to find a projection direction that effectively captures the salient features of style while maximally excluding content features. To this end, we employ Canonical Correlation Analysis (CCA) [45]. We aim to find a projection direction that maximizes the stylistic correlation between the Anchor and the Positive (F_A, F'_P) samples (rewarding style commonality), while simultaneously minimizing the content correlation between the Anchor and the Negative (F_A, F'_N) samples (penalizing content commonality). In the latent space, samples sharing the same style, such as F_A and F'_P , should be projected as closely as possible within the subspace defined by this direction. We formulate this objective of reward and penalty as a Rayleigh Quotient [10] optimization problem:

$$\operatorname{argmax}_u \rho(u) = \frac{u^T (\Sigma_{AP'} \Sigma_{P'A}) u}{u^T (\Sigma_{AA} + \lambda \Sigma_{AN'} \Sigma_{N'A}) u} \quad (8)$$

$\rho(u)$ denotes the squared correlation score. The numerator $u^T (\Sigma_{AP'} \Sigma_{P'A}) u$ measures the shared projected variance between the Anchor F_A and the semantically aligned Positive F'_P (cross-covariance reward). Since F_A and F'_P differ in content but share the same style, maximizing this term encourages projection directions that consistently capture the shared style. The denominator contains two parts. Σ_{AA} is the autocovariance of F_A , serving as a normalization metric: it keeps the quotient scale-invariant and well-posed; without this term, the denominator may become ill-conditioned or low-rank, leading to degenerate or non-

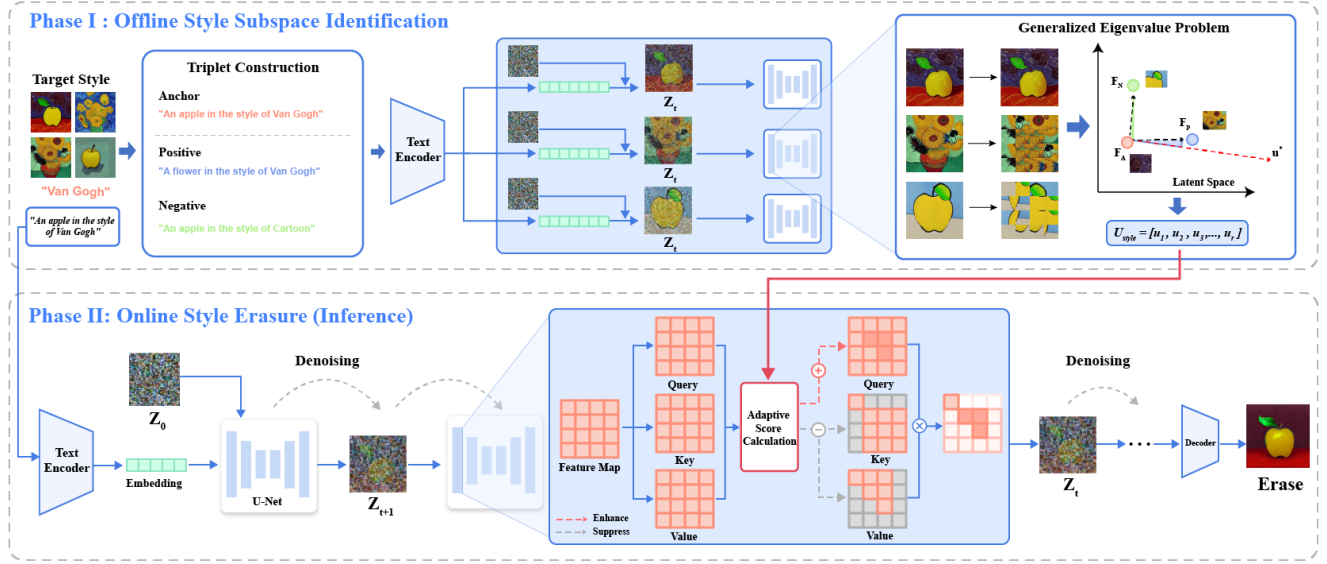


Figure 2. Overall architecture of the DICE framework. We solve a generalized eigenvalue problem on features from contrastive triplets to compute the style subspace U_{style} . During inference, the pre-computed U_{style} is used to perform Orthogonal Suppression on U-Net features, adaptively removing style components at each denoising step while preserving content.

unique solutions in the corresponding generalized eigenvalue problem. $u^T(\lambda \Sigma_{AN'} \Sigma_{N'A})u$ is a content penalty, where $\Sigma_{AN'}$ is the cross-covariance between F_A and the aligned Negative F'_N ; because F_A and F'_N share content but not style, minimizing the projected variance induced by this term suppresses directions that carry significant content information, thereby guiding the optimization towards a purer style subspace. λ is a hyperparameter that controls the strength of the content penalty.

The process of maximizing the Rayleigh quotient $\rho(u)$ is to find a projection direction u that maximally amplifies the style features while excluding the content features. Since $\rho(cu) = \rho(u)$ holds for any non-zero constant c , maximizing $\rho(u)$ is equivalent to maximizing $u^T(\Sigma_{AP'} \Sigma_{P'A})u$ under the constraint $u^T(\Sigma_{AA} + \lambda \Sigma_{AN'} \Sigma_{N'A})u = 1$. This transforms the original problem into a constrained optimization problem: Maximize:

$$u^T(\Sigma_{AP'} \Sigma_{P'A})u \quad (9)$$

Subject to:

$$u^T(\Sigma_{AA} + \lambda \Sigma_{AN'} \Sigma_{N'A})u = 1 \quad (10)$$

To solve this problem, the method of Lagrange multipliers is employed. The Lagrangian function $\mathcal{L}(u, \rho)$ is constructed as:

$$\mathcal{L}(u, \rho) = u^T(\Sigma_{AP'} \Sigma_{P'A})u - \rho(u^T(\Sigma_{AA} + \lambda \Sigma_{AN'} \Sigma_{N'A})u - 1) \quad (11)$$

Setting the gradient of \mathcal{L} with respect to u to zero yields the first-order optimality condition:

$$\nabla_u \mathcal{L} = 2(\Sigma_{AP'} \Sigma_{P'A})u - 2\rho(\Sigma_{AA} + \lambda \Sigma_{AN'} \Sigma_{N'A})u = 0 \quad (12)$$

This simplifies to the generalized eigenvalue problem:

$$(\Sigma_{AP'} \Sigma_{P'A})u = \rho(\Sigma_{AA} + \lambda \Sigma_{AN'} \Sigma_{N'A})u \quad (13)$$

Therefore, maximizing the expression of Eq. (8) is equivalent to solving the generalized eigenvalue problem in the above equation [45]. To ensure numerical stability, we consider the properties of the matrices. For any non-zero vector u , we have $u^T(\Sigma_{AP'} \Sigma_{P'A})u \geq 0$. For the denominator, we add a regularization term ϵI in our implementation to ensure it is positive definite and thus invertible, where I is the identity matrix and ϵ is a small positive number.

We solve this equation using a numerical computation library to obtain a set of eigenvalues $\rho_1 \geq \rho_2 \geq \dots \geq \rho_D$ and their corresponding eigenvectors u_1, u_2, \dots, u_D . The artistic style is typically not a single direction but a multi-factor attribute (color statistics and texture/brushstroke patterns). Therefore, we select the eigenvectors corresponding to the top r largest eigenvalues to form the style subspace:

$$U_{style} = [u_1, u_2, \dots, u_r] \in \mathbb{R}^{D \times r} \quad (14)$$

4.3. Attention Decoupling Editing

For concept erasure, a straightforward idea is to orthogonally project the patch features to remove the style component. However, this method still risks weakening content

edges while erasing style, which can lead to structural blurring in the image. Based on prior research and empirical investigation, we have observed that in the U-Net’s self-attention module, $\text{Attention}(Q, K, V)$, the K and V matrices predominantly encode specific features such as content texture and color, whereas the Q matrix encodes spatial relationships and global structure [8, 34]. Based on this insight, we propose a decoupled attention editing mechanism. Instead of editing the global attention output, we edit Q , K , and V separately. Specifically, for each token feature vector $x_i \in \mathbb{R}^{1 \times D}$ from the Key and Value matrices of the shallow network layers, we compute its coordinate vector $z_i \in \mathbb{R}^{1 \times r}$ in the basis of the style subspace $U_{style} \in \mathbb{R}^{D \times r}$:

$$z_i = x_i U_{style} \quad (15)$$

To strip the style information from the original token, we need to obtain its orthogonal projection onto the style subspace, $\text{proj}_{U_{style}}(x_i)$:

$$\text{proj}_{U_{style}}(x_i) = z_i U_{style}^T = (x_i U_{style}) U_{style}^T \quad (16)$$

Specifically, we strip the style information by subtracting this style component from the original K and V matrices, yielding the edited matrices K' and V' :

$$K' = K - \gamma \cdot \text{proj}_{U_{style}}(K) \quad (17)$$

$$V' = V - \gamma \cdot \text{proj}_{U_{style}}(V) \quad (18)$$

Here, γ is the strength parameter for erasure and suppression. By solely applying suppression to the K and V matrices, we remove style-related features such as texture and brushstrokes while minimizing damage to the content structure.

However, during the style removal process, because texture and brushstroke features are more abundant at the edges of content structures, removing these style features can also weaken content-edge information, causing content blurring. To compensate for this information loss, we repeat the process used to solve for the style subspace, but with the penalty and reward terms swapped, to solve for the content subspace $U_{content}$. $U_{content}$ is not the opposite of U_{style} ; it is obtained from a different objective that rewards $\{\text{Anchor}, \text{Negative}\}$ correlation (shared content) while penalizing $\{\text{Anchor}, \text{Positive}\}$ correlation (shared style), thus capturing complementary directions dominated by structural/layout cues.

$$\underset{w}{\text{argmax}} \quad \rho(w) = \frac{w^\top (\Sigma_{AN'} \Sigma_{N'A}) w}{w^\top (\Sigma_{AA} + \lambda \Sigma_{AP'} \Sigma_{P'A}) w} \quad (19)$$

$$(\Sigma_{AN'} \Sigma_{N'A}) w = \rho(\Sigma_{AA} + \lambda \Sigma_{AP'} \Sigma_{P'A}) w \quad (20)$$

$$U_{content} = [w_1, w_2, \dots, w_r] \in \mathbb{R}^{D \times r} \quad (21)$$

We use $U_{content}$ only to enhance Q to recover weakened content boundaries after removing style from K, V , and it does not reintroduce the erased style patterns. For the Q matrix, we project it onto the content subspace $U_{content}$ and apply a weighted addition of this content component to enhance the content:

$$Q' = Q + \gamma_q ((Q U_{content}) U_{content}^T) \quad (22)$$

where γ_q is the strength parameter for content enhancement. By performing style removal on the K and V matrices and content enhancement on the Q matrix, we feed the resulting Q', K', V' back into the U-Net to continue the denoising process:

$$\text{Attention}(Q', K', V') = \text{softmax} \left(\frac{Q' K'^T}{\sqrt{D}} \right) V' \quad (23)$$

This decoupled attention editing allows us to maximally preserve image content while removing style. We illustrate the complete algorithmic framework in Figure 2.

4.4. Adaptive Erasure Controller

During the concept erasure process, we observed that the style intensity within an image is often non-uniformly distributed. For instance, in a painting by Van Gogh, the swirling brushstrokes of the night sky exhibit a stronger style signature than static objects. When applying orthogonal suppression with a constant erasure strength, this can lead to over-erasure of content or insufficient erasure of patches with high style concentration. To address this, we designed an adaptive erasure controller that allocates the erasure strength γ according to the style concentration of each patch. To comprehensively measure the style concentration of a patch, we take each token feature vector $x_i \in \mathbb{R}^{1 \times D}$ from the shallow layers of the Q, K, V matrices, compute its coordinate vector $z_i \in \mathbb{R}^{1 \times r}$ in the basis of the style subspace $U_{style} \in \mathbb{R}^{D \times r}$ (Section 3.3), and then calculate the L2 norm of this coordinate vector as a “style score” to quantify the style concentration contained within the token:

$$s_i^{Q, K, V} = \|x_i^{Q, K, V} U_{style}\|_2 \quad (24)$$

A higher style score indicates a higher concentration of the target artistic style. Subsequently, the style scores for each component are normalized across all tokens and then combined via a weighted sum to obtain the overall style score for that patch:

$$\text{Norm}_i^{Q, K, V} = \frac{s_i^{Q, K, V}}{\max_{j=1}^N (s_j^{Q, K, V})} \quad (25)$$

$$S_i = w_q \cdot \text{Norm}_i^Q + w_k \cdot \text{Norm}_i^K + w_v \cdot \text{Norm}_i^V \quad (26)$$

Here, $w_q < w_k < w_v$ are the weight parameters for the three components, used to emphasize their different contributions to the overall style. After obtaining the patch style

Table 1. Qualitative comparison Clip score result.

	SDv1.4	SPEED	ESD-U	ESD-X	FMN	MACE	SELECT	Ours
<i>cs_{style}</i> ↓	32.138	30.385	27.521	25.837	27.426	28.112	28.938	28.827
	32.273	29.812	27.311	25.138	27.121	27.462	28.699	28.021
	33.486	30.960	27.910	26.032	27.516	27.950	29.564	28.600
	33.165	31.402	28.832	27.064	28.057	28.452	29.579	28.781
	33.377	30.972	28.157	27.056	27.819	27.820	30.189	28.272
<i>cs_{content}</i> ↑	26.052	27.838	27.229	27.933	25.695	28.551	26.522	28.561
	26.831	28.098	27.751	28.427	26.257	28.611	27.195	28.633
	25.434	26.496	26.758	27.753	23.990	27.624	26.383	28.078
	24.756	26.160	26.295	27.313	23.694	26.440	25.530	27.498
	25.998	27.211	28.232	27.944	24.858	28.108	27.595	28.642

score S_i , we use a Sigmoid function to transform it into a smooth modulation factor m_i :

$$m_i = \text{sigmoid}(k \cdot (S_i - \tau)) \quad (27)$$

where k controls the steepness of the transition and τ is the activation threshold. We define a minimum erasure strength α_{min} , and a maximum erasure strength α_{max} , to prevent insufficient and excessive erasure. Combined with the modulation factor m_i , these form the adaptive erasure strength controller:

$$\gamma = \alpha_{min} + (\alpha_{max} - \alpha_{min}) \cdot m_i \quad (28)$$

We implement soft-thresholding control via the Sigmoid function, rather than a linear mapping. Our goal is to apply a near-maximum, sufficiently strong erasure to the majority of tokens with high style concentration, while applying a minimal erasure strength to tokens with low style concentration to preserve content. By calculating the style concentration for each patch, our adaptive erasure controller can assign an appropriate erasure strength, thereby maximizing style removal while minimizing damage to the image content. This achieves precise and efficient style erasure.

5. Experiments

5.1. Implementation Details

In this section, we conduct a comprehensive evaluation of the proposed DICE framework against several baseline methods, including SPEED [23], ESD-u [11], ESD-x [11], FMN [50], MACE [27], and SELECT [53]. All our implementations use the SD v1.4 model, and all images are generated with over 100 steps. The experiments were conducted on NVIDIA RTX A6000.

Hyperparameter Settings. For style subspace estimation, we extract features from a shallow U-Net block (down_blocks[0]) and solve the proposed contrastive objective with the content penalty weight $\lambda = 1.0$. We compute a content subspace $U_{content}$ analogously from features extracted at up_blocks[3], using $\lambda = 1.0$ and apply it only to enhance the Query matrix with strength $\gamma_q = 0.25$.

Table 2. Qualitative comparison DLPIPS result.

	SDv1.4	SPEED	ESD-U	ESD-X	FMN	MACE	SELECT	Ours
L_{gene} ↑	0.7141	0.737	0.855	0.868	0.877	0.764	0.694	0.860
	0.7358	0.767	0.868	0.891	0.931	0.804	0.715	0.867
C_{style} ↑	0.56953	0.077	0.314	0.282	0.264	0.110	0.105	0.272
	0.58752	0.047	0.285	0.259	0.251	0.101	0.099	0.256
$C_{content}$ ↓	0.85857	0.009	-0.018	-0.011	-0.023	0.025	-0.042	-0.133
	0.84696	-0.015	0.069	0.050	0.054	-0.008	-0.004	-0.027

5.2. Evaluation Metrics

5.2.1. Clip Score

We have designed five groups of prompts specifically for the artist’s style and content. The two types of prompts each only contain target style and content, in order to prevent the Clip Score[32] from being unable to accurately evaluate due to the excessive disruption of the content and style differences. We use this refined template design to separately assess the thoroughness of the art style erasure(*cs_{style}*) and the completeness of the content retention(*cs_{content}*).

5.2.2. Differential-LPIPS

Learned Perceptual Image Patch Similarity (LPIPS) [51] is used to measure the difference between two images in the perceptual feature space. A larger value indicates a greater perceptual difference between the two images. Traditional LPIPS can only provide the overall perceptual difference between two images, without distinguishing whether this difference originates from style erasure or content degradation. We proposed the Differential-LPIPS (DLPIPS). By calculating the differences between each pair of samples to measure the perceived differences, the evaluation of erasure performance is conducted from three dimensions:

Erasure Generalization. Generate the reference image I_{ref}^{gene} using a variant of the original prompt. Calculate the LPIPS score L_{gene} between the erased image I_{erase} and I_{ref}^{gene} . When L_{erase} is larger, it indicates that although there are slight changes in the expression, the scheme can still generalize the erasure effect to a fixed artist style.

Erasure Effectiveness. Using prompts of different content but with the same style to generate reference image I_{ref}^{style} , calculate the LPIPS (L_{base}^{style}) of original image I_{ori} and I_{ref}^{style} as the baseline, which measures the perceptual difference caused by the different content. we calculate the LPIPS (L_{base}^{style}) of I_{erase} and I_{ref}^{style} , obtaining C_{style} :

$$C_{style} = L_{erase}^{style} - L_{base}^{style} \quad (29)$$

This difference measures the additional perceptual distance caused by removing the common style. The larger the C_{style} , the more thorough the erasure.

Content Preservation. Content Preservation focuses on the degree of content preservation during the erasure process. We generate a reference image I_{ref}^{cont} and calculate its LPIPS score (L_{base}^{cont}) with the original image I_{ori} as a

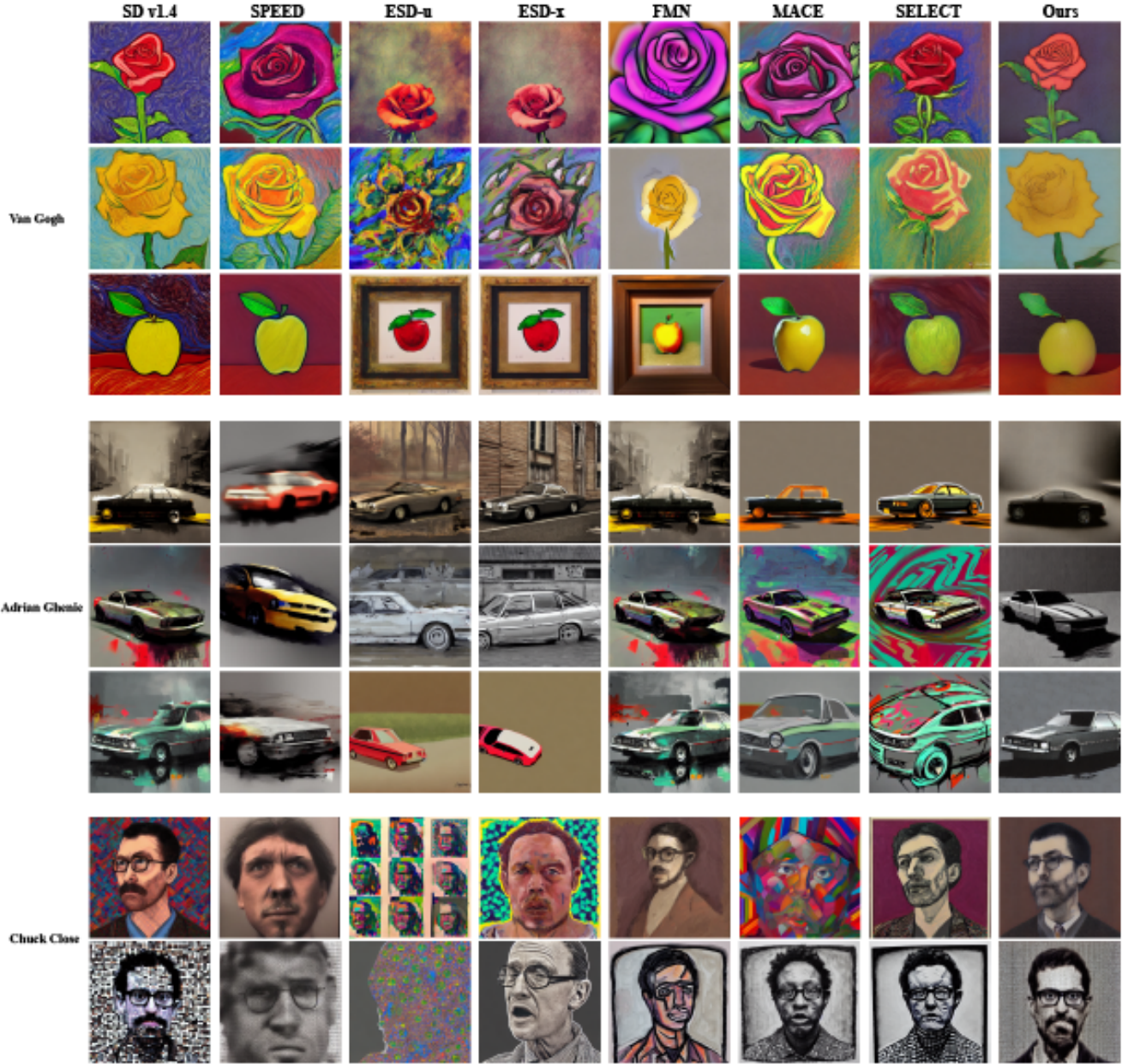


Figure 3. Qualitative comparison for erasing the "Van Gogh", "Adrian Ghenie", "Chuck Close" artistic style. Our method demonstrates superior performance by completely removing stylistic features (e.g., swirling brushstrokes and specific color palettes) while best preserving the content structure. In contrast, other baseline methods exhibit issues such as residual style, severe content degradation, or the introduction of irrelevant artifacts.

baseline. This baseline measures the perceptual difference caused by the different styles. Subsequently, we calculate the LPIPS score ($L_{\text{erase}}^{\text{cont}}$) between the reference image $I_{\text{ref}}^{\text{cont}}$ and the erased image I_{erase} . To better measure the additional content degradation introduced during the erasure process, we calculate the difference:

$$C_{\text{content}} = L_{\text{erase}}^{\text{cont}} - L_{\text{base}}^{\text{cont}} \quad (30)$$

This difference value measures the additional perceptual difference potentially caused by content loss from removing the common style. To make the metric more stable and robust, we use multiple reference styles to average the baseline. To validate this metric more intuitively, we provide an example in Supp A.2.2.

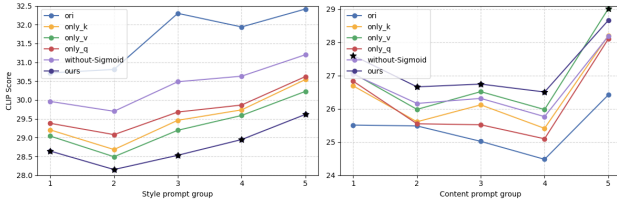


Figure 4. Quantitative CLIP Score evaluation for the ablation study of the AEC. The left sub-figure reports cs_{style} computed on five style-only prompt templates (lower is better). The right sub-figure reports $cs_{content}$ computed on five content-only prompt templates, measuring content retention (higher is better).

Table 3. Adaptive Erasure Controller ablation (DLPIPS). Higher L_{gene}/C_{style} and lower $C_{content}$ are better.

	SDv1.4(L_{base})	only.k	only.v	only.q	without-Sigmoid	Ours
Original↑	—	0.572	0.603	0.5357	0.531	0.610
$L_{gene} \uparrow$	0.3509	0.633	0.681	0.579	0.581	0.673
	0.4023	0.631	0.649	0.592	0.591	0.664
$C_{style} \uparrow$	0.5613	0.188	0.214	0.150	0.144	0.221
	0.4864	0.200	0.239	0.177	0.154	0.251
$C_{content} \downarrow$	0.7720	-0.058	-0.014	-0.063	-0.020	-0.055
	0.83101	-0.027	-0.013	-0.012	0.001	-0.043

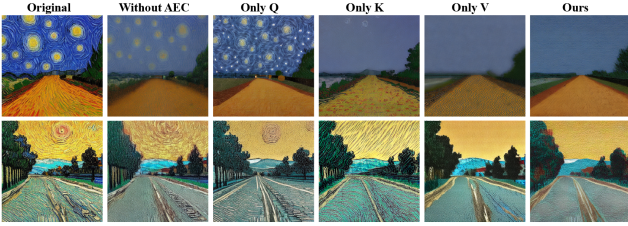


Figure 5. Qualitative ablation of the Adaptive Erasure Controller. The experiment shows that the combination of the fusion calculation of Q , K , V and nonlinear control is crucial for eliminating the style while preserving the content.

5.3. Standard Performance Evaluation

We evaluate the erasure of the three artist style, with the results shown in Figure 3. Our method uniquely removes stylistic features (e.g., brushstrokes, color palettes) while preserving clean, natural content. In contrast, other baseline methods either fail to completely erase the style or introduce severe content corruption.

This observation is validated by quantitative metrics. As shown in Table 1, while methods like ESD-x achieve the lowest Clip Score (cs_{style}), this comes at the cost of significant content degradation. Our method strikes a superior balance, achieving the highest content preservation score ($cs_{content}$) while maintaining a competitive style erasure effect. To distinguish precise erasure from general image degradation (i.e., severe content destruction), we employ our proposed DLPIPS metric for evaluation (Table 2). In contrast to the Clip Score, FMN [50] and ESD-u [11]

Table 4. The ablation experiment results of the DLPIPS indicators for the ADE module.

	SDv1.4(L_{base})	without Q	QKV -befor	QKV -Mixed	Ours
$C_{style} \uparrow$	0.605	0.109	0.158	0.101	0.098
	0.641	0.087	0.102	0.060	0.069
$C_{content} \downarrow$	0.667	0.085	0.134	0.043	0.052
	0.825	0.007	0.017	0.013	0.001
$H_o \uparrow$	—	0.052	0.054	0.052	0.057



Figure 6. Qualitative ablation study for ADE. The results demonstrated that indiscriminate inhibition of Q , K and V failed to preserve the content.

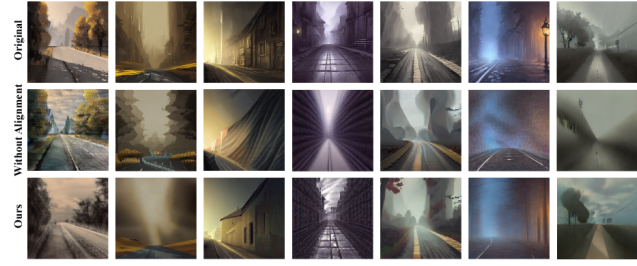


Figure 7. Qualitative ablation study for Token Alignment. Token alignment is shown to be critical for preventing structural distortions by ensuring an accurate style difference computation.

achieve the highest difference scores for erasure generalization and thoroughness. However, their content preservation scores are suboptimal. This indicates that while both our method and several baselines achieve style erasure, the other approaches do so by sacrificing content integrity in exchange for perceptual distance from the original style. Our method implements a purifying form of erasure that not only precisely strips the target artist’s style but also actively restores the core content affected by it.

5.4. Ablations

5.4.1. Adaptive Erasure Controller

Adaptive Erasure Controller module performs a weighted summation of the style scores from Q , K , and V , and uses a Sigmoid function to achieve adaptive control for different regions. The four ablation variants we designed are: using only K , only V , or only Q to calculate the style score, and removing the Sigmoid function. The results are presented

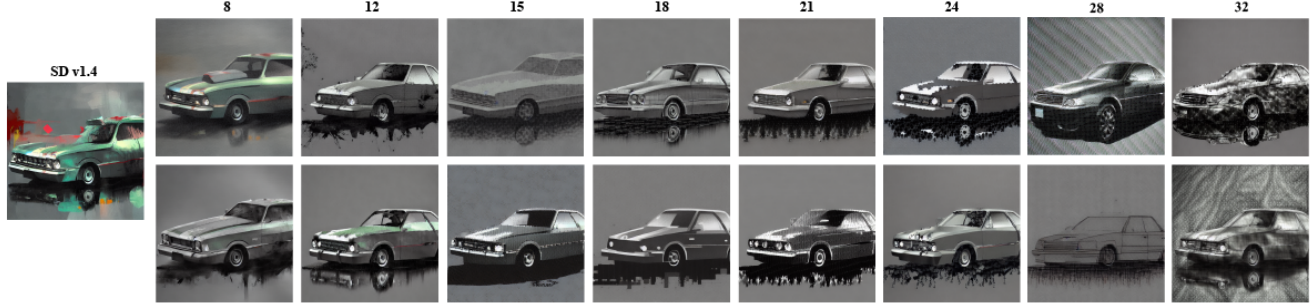


Figure 8. Style subspace dimension sensitivity. Small r retains artist-specific color and brush traits; large r introduces high-frequency artifacts. The mid-range [12,21] consistently achieves clean style removal with high content fidelity.



Figure 9. Qualitative ablation study on the diffusion step interval for feature extraction.

in Figure 4, 5, and Table 3. The proposed Adaptive Erasure Controller demonstrates superior performance across multiple metrics and visual evaluations. Using a uniform erasure strength (Without AEC) leads to incomplete removal, rotating brushstrokes on the ground or trees may be weakened, but strong strokes in the sky background persist. This indicates that different spatial patches exhibit different style intensities and therefore require adaptive erasure strengths. Variants that compute style scores using only Q, only K, or only V all show incomplete erasure. Our full approach achieves clean and thorough removal of style for each content instance while maximally preserving road geometry, tree morphology, and distant architectural details.

5.4.2. Attention decoupling editing

We designed three ablation variants: suppressing style in only K and V (Without Q); suppressing Q, K, and V before the self-attention computation (QKV-before); and applying suppression after the self-attention computation (QKV-Mixed). Figure 6 and Table 4 present the results. The “Without Q strength” variant removes artistic style to some extent, but causes substantial damage to content and structure; objects, layout, and composition undergo pronounced changes, whereas our method removes style while maximally retaining the original content arrangement. Deter-

ministic evaluation with DPLIPS indicates that “QKV - before” with “without Q strength” reveals that “QKV - before” merely lacks the content-preserving operation of Q; while it improves style erasure, it incurs greater content damage. From this, it can be seen that Q also has style characteristics, but it mainly carries content information. To assess the joint objective, we use the holistic index $H_o = C_{style} - C_{content}$. Our full method achieves the highest, confirming that our differentiated approach, reinforcing content via Q while stripping style from K and V, delivers precise style erasure with maximal content fidelity.

5.4.3. Token Alignment

We conducted an ablation study to investigate the effect of our token alignment operation. we present the ablation experiment results of whether to use token alignment (Figure 7). The variant without token alignment produces images with blurry color patches and distorted structures. When the style difference cannot be accurately computed, the method not only fails to thoroughly erase the style but also damages the content’s structure.

5.5. Hyperparameter Sensitivity

To verify the impact of key hyperparameters on the robustness of our method, we conduct sensitivity tests on three

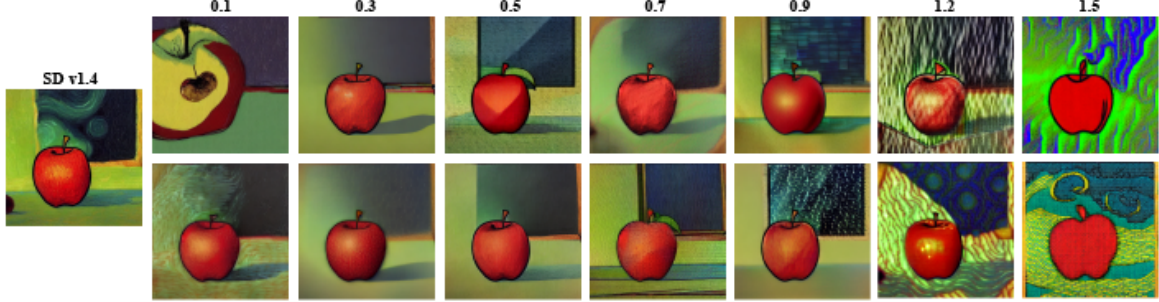


Figure 10. Sensitivity test of the Q content enhancement coefficient γ_q . Within the range [0.3, 0.9], the method exhibits higher-quality style erasure and content preservation.

groups of hyperparameters while keeping all other settings unchanged, including the spatial dimension r for capturing the style subspace, the diffusion step interval s for feature extraction, and the coefficient γ_q for Q-based content enhancement.

5.5.1. Style Subspace Dimension

The spatial dimension r for capturing the style subspace defines the number of eigenvectors in U_{style} . We establish eight test settings $\{8, 12, 15, 18, 21, 24, 28, 32\}$, and present the results in Figure 8. We observe that when the dimension used to capture the style subspace is too low, although salient brushstrokes and exaggerated color schemes are suppressed, residual style textures remain in the environment beneath the car, and parts of the color patterns are not removed, indicating that a small r cannot cover the diversity of the artist’s style and thus leads to residual style. In the $\{12, 15, 18, 21\}$ dimension range, the method exhibits superior completeness of style removal and preservation of content: the brushstroke textures and color patterns annotated in both background and foreground are thoroughly suppressed, while structural information is well preserved. When r is further increased, additional textures and artifacts become evident in the background and near the car underbody, indicating that a large r introduces too many noise features and causes visual degradation.

5.5.2. Feature Extraction Diffusion Interval

We investigated the sensitivity to the diffusion step interval for extracting feature maps to solve for the style subspace. We extracted feature maps from multiple diffusion step intervals and performed the same inference, with the results shown in Figure 9. It can be observed that inference using features from early diffusion intervals results in abstract textures and artifacts. In contrast, extracting feature maps from steps 0-400 not only effectively erases the artistic style but also preserves the main structure and details of the content. This demonstrates that selecting an appropriate feature extraction interval is crucial, as it provides the most effective and separable features for our method.

5.5.3. Q Content Enhancement Intensity

The content enhancement coefficient γ_q for vector Q acts directly on the additive content component of the Query:

$$\mathbf{Q}' = \mathbf{Q} + \gamma_q((\mathbf{Q}\mathbf{U}_{content})\mathbf{U}_{content}^T) \quad (31)$$

We test seven coefficient values in the range [0.1, 0.3, 0.5, 0.7, 0.9, 1.2, 1.5], covering settings from weak guidance to strong guidance. The experimental results are presented in Figure 10. We observe that low-strength Q content enhancement yields insufficient preservation of content structure, leading to deformation of the apple contour. Within the range [0.3, 0.9], the erased images exhibit relatively stable content structure; the primary object shape is preserved, and the style is effectively removed. At larger γ_q , additional chaotic color banding is introduced, producing artifacts. Consequently, the Q content enhancement strength γ_q exhibits a clear effective interval within which style erasure and content preservation are superior and insensitive to the precise strength, demonstrating the robustness of our method.

6. Conclusion

We propose DICE, a training-free, inference-time framework. Our method implements a purified style erasure, which achieves the decoupling of content and style by accurately capturing specific stylistic features and enables precise style erasure through fine-grained differential editing techniques. Our algorithm demonstrates the complete preservation of content information (such as object morphology, scene layout, and structural perspective). In the processed images, not only is the style thoroughly removed, but no additional textures or chaotic content are introduced. This illustrates that our method achieves efficient decoupling of content and style in the latent space, which is the key to our algorithm’s precise editing capabilities. Although our research is oriented towards artist style erasure, its core technology demonstrates the ability to perform precise, targeted editing of highly entangled and abstract visual con-

cepts within generative models.

References

- [1] Sk Miraj Ahmed, Umit Yigit Basaran, Dripta S Raychaudhuri, Arindam Dutta, Rohit Kundu, Fahim Faisal Niloy, Basak Guler, and Amit K Roy-Chowdhury. Towards source-free machine unlearning. In *Proceedings of the Computer Vision and Pattern Recognition Conference*, pages 4948–4957, 2025. 3
- [2] Namhyuk Ahn, KiYoon Yoo, Wonhyuk Ahn, Daesik Kim, and Seung-Hun Nam. Nearly zero-cost protection against mimicry by personalized diffusion models. In *Proceedings of the Computer Vision and Pattern Recognition Conference*, pages 28801–28810, 2025. 3
- [3] Samyadeep Basu, Nanxuan Zhao, Vlad I Morariu, Soheil Feizi, and Varun Manjunatha. Localizing and editing knowledge in text-to-image generative models. In *The Twelfth International Conference on Learning Representations*, 2023. 5
- [4] Anh Bui, Trang Vu, Long Vuong, Trung Le, Paul Montague, Tamas Abraham, Junae Kim, and Dinh Phung. Fantastic targets for concept erasure in diffusion models and where to find them. *arXiv preprint arXiv:2501.18950*, 2025. 1
- [5] Ruchika Chavhan, Da Li, and Timothy Hospedales. Conceptprune: Concept editing in diffusion models via skilled neuron pruning. *arXiv preprint arXiv:2405.19237*, 2024. 3
- [6] Die Chen, Zhiwen Li, Mingyuan Fan, Cen Chen, Wenmeng Zhou, Yanhao Wang, and Yaliang Li. Growth inhibitors for suppressing inappropriate image concepts in diffusion models. *arXiv preprint arXiv:2408.01014*, 2024. 1, 3
- [7] Liang Chen, Haozhe Zhao, Tianyu Liu, Shuai Bai, Junyang Lin, Chang Zhou, and Baobao Chang. An image is worth 1/2 tokens after layer 2: Plug-and-play inference acceleration for large vision-language models. In *European Conference on Computer Vision*, pages 19–35. Springer, 2024. 4
- [8] Jiwoo Chung, Sangeek Hyun, and Jae-Pil Heo. Style injection in diffusion: A training-free approach for adapting large-scale diffusion models for style transfer. In *Proceedings of the IEEE/CVF conference on computer vision and pattern recognition*, pages 8795–8805, 2024. 7
- [9] Masud An Nur Islam Fahim, Nazmus Saqib, and Jani Boutellier. Stam: Zero-shot style transfer using diffusion model via attention modulation. In *Proceedings of the Computer Vision and Pattern Recognition Conference*, pages 6333–6343, 2025. 3
- [10] Ronald A Fisher. The use of multiple measurements in taxonomic problems. *Annals of eugenics*, 7(2):179–188, 1936. 5
- [11] Rohit Gandikota, Joanna Materzynska, Jaden Fiotto-Kaufman, and David Bau. Erasing concepts from diffusion models. In *Proceedings of the IEEE/CVF international conference on computer vision*, pages 2426–2436, 2023. 2, 8, 10, 17, 18
- [12] Daiheng Gao, Shilin Lu, Wenbo Zhou, Jiaming Chu, Jie Zhang, Mengxi Jia, Bang Zhang, Zhaoxin Fan, and Weiming Zhang. Eraseanything: Enabling concept erasure in rectified flow transformers. In *Forty-second International Conference on Machine Learning*, 2025. 1
- [13] Chao Gong, Kai Chen, Zhipeng Wei, Jingjing Chen, and Yu-Gang Jiang. Reliable and efficient concept erasure of text-to-image diffusion models. In *European Conference on Computer Vision*, pages 73–88. Springer, 2024. 1
- [14] Feihong He, Gang Li, Fuhui Sun, Mengyuan Zhang, Lingyu Si, Xiaoyan Wang, and Li Shen. Freestyle: Free lunch for text-guided style transfer using diffusion models. *Pattern Recognition*, page 113093, 2026. 3
- [15] Alvin Heng and Harold Soh. Selective amnesia: A continual learning approach to forgetting in deep generative models. *Advances in Neural Information Processing Systems*, 36: 17170–17194, 2023. 2
- [16] Amir Hertz, Ron Mokady, Jay Tenenbaum, Kfir Aberman, Yael Pritch, and Daniel Cohen-Or. Prompt-to-prompt image editing with cross attention control. *arXiv preprint arXiv:2208.01626*, 2022. 3, 5
- [17] Jonathan Ho and Tim Salimans. Classifier-free diffusion guidance. *arXiv preprint arXiv:2207.12598*, 2022. 4
- [18] Seunghoo Hong, Juhun Lee, and Simon S Woo. All but one: Surgical concept erasing with model preservation in text-to-image diffusion models. In *Proceedings of the AAAI Conference on Artificial Intelligence*, pages 21143–21151, 2024. 2
- [19] Chi-Pin Huang, Kai-Po Chang, Chung-Ting Tsai, Yung-Hsuan Lai, Fu-En Yang, and Yu-Chiang Frank Wang. Receler: Reliable concept erasing of text-to-image diffusion models via lightweight erasers. In *European Conference on Computer Vision*, pages 360–376. Springer, 2024. 2
- [20] Changhoon Kim, Kyle Min, and Yezhou Yang. Race: Robust adversarial concept erasure for secure text-to-image diffusion model. In *European Conference on Computer Vision*, pages 461–478. Springer, 2024. 2
- [21] Sanghyun Kim, Seohyeon Jung, Balhae Kim, Moonseok Choi, Jinwoo Shin, and Juho Lee. Safeguard text-to-image diffusion models with human feedback inversion. In *European Conference on Computer Vision*, pages 128–145. Springer, 2024. 2
- [22] Byung Hyun Lee, Sungjin Lim, and Se Young Chun. Localized concept erasure for text-to-image diffusion models using training-free gated low-rank adaptation. In *Proceedings of the Computer Vision and Pattern Recognition Conference*, pages 18596–18606, 2025. 3
- [23] Ouxiang Li, Yuan Wang, Xinting Hu, Houcheng Jiang, Tao Liang, Yanbin Hao, Guojun Ma, and Fuli Feng. Speed: Scalable, precise, and efficient concept erasure for diffusion models. *arXiv preprint arXiv:2503.07392*, 2025. 1, 3, 8, 17, 18
- [24] Zhiwen Li, Die Chen, Mingyuan Fan, Cen Chen, Yaliang Li, Yanhao Wang, and Wenmeng Zhou. Responsible diffusion models via constraining text embeddings within safe regions. In *Proceedings of the ACM on Web Conference 2025*, pages 1588–1601, 2025. 1, 3
- [25] Yizhou Lin, Nisha Huang, Kaer Huang, Henglin Liu, Yiqiang Yan, Jie Guo, Tong-Yee Lee, and Xiu Li. Ice: Intercede concept erasure in text-to-image diffusion models. In *Proceedings of the 33rd ACM International Conference on Multimedia*, pages 11328–11336, 2025. 1

[26] Renyang Liu, Kangjie Chen, Han Qiu, Jie Zhang, Kwok-Yan Lam, Tianwei Zhang, and See-Kiong Ng. Saferedir: Prompt embedding redirection for robust unlearning in image generation models. *arXiv preprint arXiv:2601.08623*, 2026. 3

[27] Shilin Lu, Zilan Wang, Leyang Li, Yanzhu Liu, and Adams Wai-Kin Kong. Mace: Mass concept erasure in diffusion models. In *Proceedings of the IEEE/CVF Conference on Computer Vision and Pattern Recognition*, pages 6430–6440, 2024. 1, 8, 17, 18

[28] Mengyao Lyu, Yuhong Yang, Haiwen Hong, Hui Chen, Xuan Jin, Yuan He, Hui Xue, Jungong Han, and Guiguang Ding. One-dimensional adapter to rule them all: Concepts diffusion models and erasing applications. In *Proceedings of the IEEE/CVF Conference on Computer Vision and Pattern Recognition*, pages 7559–7568, 2024. 2

[29] Muhammad Shahid Munneer and Simon S Woo. Towards safe synthetic image generation on the web: A multimodal robust nsfw defense and million scale dataset. In *Companion Proceedings of the ACM on Web Conference 2025*, pages 1209–1213, 2025. 1

[30] Kien Nguyen, Anh Tran, and Cuong Pham. Suma: A subspace mapping approach for robust and effective concept erasure in text-to-image diffusion models. In *Proceedings of the IEEE/CVF International Conference on Computer Vision*, pages 19587–19596, 2025. 2, 3

[31] Josephine Passananti, Stanley Wu, Shawn Shan, Haitao Zheng, and Ben Y Zhao. Disrupting style mimicry attacks on video imagery. *arXiv preprint arXiv:2405.06865*, 2024. 3

[32] Alec Radford, Jong Wook Kim, Chris Hallacy, Aditya Ramesh, Gabriel Goh, Sandhini Agarwal, Girish Sastry, Amanda Askell, Pamela Mishkin, Jack Clark, et al. Learning transferable visual models from natural language supervision. In *International conference on machine learning*, pages 8748–8763. PMLR, 2021. 8

[33] Robin Rombach, Andreas Blattmann, Dominik Lorenz, Patrick Esser, and Björn Ommer. High-resolution image synthesis with latent diffusion models. In *Proceedings of the IEEE/CVF conference on computer vision and pattern recognition*, pages 10684–10695, 2022. 4

[34] Viraj Shah, Nataniel Ruiz, Forrester Cole, Erika Lu, Svetlana Lazebnik, Yuanzhen Li, and Varun Jampani. Ziplora: Any subject in any style by effectively merging loras. In *European Conference on Computer Vision*, pages 422–438. Springer, 2024. 7

[35] Shawn Shan, Jenna Cryan, Emily Wenger, Haitao Zheng, Rana Hanocka, and Ben Y Zhao. Glaze: Protecting artists from style mimicry by {Text-to-Image} models. In *32nd USENIX Security Symposium (USENIX Security 23)*, pages 2187–2204, 2023. 1, 3

[36] Shawn Shan, Wenxin Ding, Josephine Passananti, Stanley Wu, Haitao Zheng, and Ben Y Zhao. Nightshade: Prompt-specific poisoning attacks on text-to-image generative models. In *2024 IEEE Symposium on Security and Privacy (SP)*, pages 807–825. IEEE, 2024. 3

[37] Peter Shaw, Jakob Uszkoreit, and Ashish Vaswani. Self-attention with relative position representations. *arXiv preprint arXiv:1803.02155*, 2018. 4

[38] Jiaming Sun, Zehong Shen, Yuang Wang, Hujun Bao, and Xiaowei Zhou. Loftr: Detector-free local feature matching with transformers. In *Proceedings of the IEEE/CVF conference on computer vision and pattern recognition*, pages 8922–8931, 2021. 5

[39] Raphael Tang, Crystina Zhang, Lixin Xu, Yao Lu, Wenyan Li, Pontus Stenetorp, Jimmy Lin, and Ferhan Türe. Words worth a thousand pictures: Measuring and understanding perceptual variability in text-to-image generation. In *Proceedings of the 2024 Conference on Empirical Methods in Natural Language Processing*, pages 5441–5454, 2024. 4

[40] Narek Tumanyan, Michal Geyer, Shai Bagon, and Tali Dekel. Plug-and-play diffusion features for text-driven image-to-image translation. In *Proceedings of the IEEE/CVF conference on computer vision and pattern recognition*, pages 1921–1930, 2023. 5

[41] Jack Urbanek, Florian Bordes, Pietro Astolfi, Mary Williamson, Vasu Sharma, and Adriana Romero-Soriano. A picture is worth more than 77 text tokens: Evaluating clip-style models on dense captions. In *Proceedings of the IEEE/CVF Conference on Computer Vision and Pattern Recognition*, pages 26700–26709, 2024. 2

[42] Jiayu Wang, Yifei Ming, Zhenmei Shi, Vibhav Vineet, Xin Wang, Sharon Li, and Neel Joshi. Is a picture worth a thousand words? delving into spatial reasoning for vision language models. *Advances in Neural Information Processing Systems*, 37:75392–75421, 2024. 2

[43] Ruipeng Wang, Junfeng Fang, Jiaqi Li, Hao Chen, Jie Shi, Kun Wang, and Xiang Wang. Ace: Concept editing in diffusion models without performance degradation. In *Proceedings of the 33rd ACM International Conference on Multimedia*, pages 10525–10534, 2025. 1

[44] Yuan Wang, Ouxiang Li, Tingting Mu, Yanbin Hao, Kuien Liu, Xiang Wang, and Xiangnan He. Precise, fast, and low-cost concept erasure in value space: Orthogonal complement matters. In *2025 IEEE/CVF Conference on Computer Vision and Pattern Recognition (CVPR)*, pages 28759–28768. IEEE, 2025. 1

[45] David Weenink. Canonical correlation analysis. In *Proceedings of the Institute of Phonetic Sciences of the University of Amsterdam*, pages 81–99. University of Amsterdam Amsterdam, 2003. 4, 5, 6

[46] Ju-Hsuan Weng, Jia-Wei Liao, Cheng-Fu Chou, and Jun-Cheng Chen. Multimodal robustness benchmark for concept erasure in diffusion models. In *Generative and Protective AI for Content Creation*, 2024. 3

[47] Jing Wu, Trung Le, Munawar Hayat, and Mehrtash Harandi. Erasing undesirable influence in diffusion models. In *Proceedings of the Computer Vision and Pattern Recognition Conference*, pages 28263–28273, 2025. 2

[48] Lexiang Xiong, Chengyu Liu, Jingwen Ye, Yan Liu, and Yuecong Xu. Semantic surgery: Zero-shot concept erasure in diffusion models. *arXiv preprint arXiv:2510.22851*, 2025. 3

[49] Tianyun Yang, Juan Cao, and Chang Xu. Pruning for robust concept erasing in diffusion models. *arXiv preprint arXiv:2405.16534*, 2024. 3

- [50] Gong Zhang, Kai Wang, Xingqian Xu, Zhangyang Wang, and Humphrey Shi. Forget-me-not: Learning to forget in text-to-image diffusion models. In *Proceedings of the IEEE/CVF conference on computer vision and pattern recognition*, pages 1755–1764, 2024. 8, 10, 17, 18
- [51] Richard Zhang, Phillip Isola, Alexei A Efros, Eli Shechtman, and Oliver Wang. The unreasonable effectiveness of deep features as a perceptual metric. In *Proceedings of the IEEE conference on computer vision and pattern recognition*, pages 586–595, 2018. 8
- [52] Siyuan Zhang, Wei Ma, Libin Liu, Zheng Li, and Hongbin Zha. Training-free fourier phase diffusion for style transfer. In *Proceedings of the Thirty-Fourth International Joint Conference on Artificial Intelligence*, pages 2386–2394, 2025. 3
- [53] Tong Zhang, Ru Zhang, Jianyi Liu, Zhen Yang, and Gongshen Liu. Beyond fixed anchors: Precisely erasing concepts with sibling exclusive counterparts. *arXiv preprint arXiv:2510.16342*, 2025. 2, 3, 4, 8, 17, 18
- [54] Yang Zhang, Er Jin, Yanfei Dong, Yixuan Wu, Philip Torr, Ashkan Khakzar, Johannes Stegmaier, and Kenji Kawaguchi. Minimalist concept erasure in generative models. *arXiv preprint arXiv:2507.13386*, 2025. 1

DICE: Disentangling Artist Style from Content via Contrastive Subspace Decomposition in Diffusion Models

Supplementary Material

A. Evaluation Metrics

In the artist style erasure process, we aim to evaluate three dimensions:

- Can the algorithm generalize the erasure effect to fixed artist styles?
- How thoroughly is the style erased in the post-erasure image compared to the original style?
- How much of the original content is preserved during style erasure?

In addition to visual verification, we employed two metrics for evaluation: Clip Score and LPIPS.

A.1. CLIP Score

We adopt Clip Score to verify the completeness of erasure and the retention of content, and different from previous studies, we design a more refined cs score evaluation criterion. We design five sets of prompt respectively for artist style and content. The artist style prompt only includes target style, but does not include content involved in reasoning, so as to avoid the cs score being dominated by content and producing a high score, which cannot accurately evaluate the completeness of style erasure. Similarly, the content prompt contains only content. We use this refined template design to separately evaluate artistic style erasure thoroughness and content retention completeness. We provide a set of examples in Table S5 where the user enters "A road in the style of Van Gogh".

Table S5. Example prompts for Style and Content evaluation.

Category	Prompt
Style	<ol style="list-style-type: none"> 1. "A work in the style of Van Gogh" 2. "A creation in the style of Van Gogh" 3. "Artwork in the style of Vincent van Gogh" 4. "Painting in the style of Van Gogh" 5. "An image with the artistic style of Van Gogh"
Content	<ol style="list-style-type: none"> 6. "A road" 7. "A picture of a road" 8. "An image showing a road" 9. "A photograph of a road" 10. "A scene with a road"

A.2. DLPIPS

LPIPS approximates human perceptual differences by feeding images into a pre-trained network, extracting multi-layer features, and calculating a weighted distance in the

feature space. A larger value indicates a greater perceptual difference between the two images. Traditional LPIPS can only provide the overall perceptual difference between two images, without distinguishing whether this difference originates from style erasure or content degradation. To address this issue, we propose the Differential-LPIPS (DLPIPS), a metric that constructs baselines using multiple sets of reference images. By calculating the differences between these LPIPS scores, it evaluates erasure performance across three dimensions: **Erasure Generalization**, **Erasure Effectiveness**, and **Content Preservation**. It is important to note that we do not assume linear additivity for LPIPS. Instead, we regard these differences as an approximate measure of the additional perceptual cost incurred by the variation of a specific factor under a given reference baseline.

The original image be denoted as I_{ori} , and the style-erased image as I_{erase} . Let $\text{LPIPS}(I, J)$ represent the LPIPS distance between two images I and J . In DLPIPS, we construct three types of reference samples by slightly modifying the original prompts: a generalization sample ($I_{\text{ref}}^{\text{gene}}$) that is semantically similar but still contains the target style, a style sample ($I_{\text{ref}}^{\text{style}}$) that has different content but shares the same target style, and a content reference image ($I_{\text{ref}}^{\text{cont}}$) that has the same content but does not contain the target style, approaching a neutral style.

A.2.1. Erasure Generalization

Erasure Generalization focuses on whether the erasure solution can still generalize to the fixed artist's style when the prompt undergoes minor modifications (similar semantics, unchanged style) (e.g., modifying {A road in the style of Van Gogh} to {A path in the style of Vincent Willem van Gogh}). We generate a reference image $I_{\text{ref}}^{\text{gene}}$ from the modified prompt and calculate its LPIPS score with the erased image I_{erase} :

$$L_{\text{gene}} = \text{LPIPS}(I_{\text{ref}}^{\text{gene}}, I_{\text{erase}}) \quad (\text{S32})$$

A larger L_{gene} indicates a more thorough erasure, suggesting that despite minor changes in the prompt, the solution can still generalize the erasure effect to the fixed artist's style, achieving a more complete erasure.

A.2.2. Erasure Effectiveness

Erasure Effectiveness focuses on the degree of style difference reduced by the erasure operation compared to the original image, thereby measuring the thoroughness of the erasure. We generate a reference image $I_{\text{ref}}^{\text{style}}$ and calculate its LPIPS score with the original image I_{ori} as a baseline. This



Figure S11. Quantitative results for erasing “Van Gogh” and preserving “rose”. (SPEED[23], ESD-x[11], ESD-u[11], FMN[50], MACE[27], SELECT[53]). In the second row, we provide the average $L_{\text{cont}}^{\text{erase}}$ score for each group. Red indicates solutions with $C_{\text{content}} < 0$, and blue indicates $C_{\text{content}} > 0$. We have also marked in the figure the images where the style is erased and the content is well-preserved (marked with a green checkmark). We observe that for solutions that erase cleanly and preserve content well, C_{content} is consistently significantly less than 0 (“SELECT” and “Ours”). For solutions that erase the style thoroughly but where the content structure and layout are damaged, C_{content} is significantly greater than 0. Crucially, in the third-row samples for the SPEED and MACE solutions, an erasure failure occurred; the rotating brushstrokes in the background are still not completely erased, but the content is well-preserved. Their C_{content} values of $-0.003/0.009$ are very close to 0.

baseline measures the perceptual difference caused by the different content:

$$L_{\text{base}}^{\text{style}} = \text{LPIPS}(I_{\text{ref}}^{\text{style}}, I_{\text{ori}}) \quad (\text{S33})$$

Subsequently, we calculate the LPIPS score between the erased image I_{erase} and the reference image $I_{\text{ref}}^{\text{style}}$:

$$L_{\text{erase}}^{\text{style}} = \text{LPIPS}(I_{\text{ref}}^{\text{style}}, I_{\text{erase}}) \quad (\text{S34})$$

The difference is calculated as:

$$C_{\text{style}} = L_{\text{erase}}^{\text{style}} - L_{\text{base}}^{\text{style}} \quad (\text{S35})$$

This difference measures the additional perceptual distance gained from removing the common style. When the erasure fails, I_{erase} is close to I_{ori} , and C_{style} approaches 0. The more thorough the erasure, the more the appearance of I_{erase} deviates from the artistic style, making $L_{\text{erase}}^{\text{style}}$ significantly larger than the baseline $L_{\text{base}}^{\text{style}}$, and thus resulting in a larger C_{style} . When comparing multiple baseline methods, a larger C_{style} indicates a more thorough erasure.

A.2.3. Content Preservation

Content Preservation focuses on the degree of content preservation during the erasure process. An ideal erasure operation should only remove style features, preserving the

content structure and semantic information as much as possible. We generate a reference image $I_{\text{ref}}^{\text{cont}}$ and calculate its LPIPS score with the original image I_{ori} as a baseline. This baseline measures the perceptual difference caused by the different styles:

$$L_{\text{base}}^{\text{cont}} = \text{LPIPS}(I_{\text{ref}}^{\text{cont}}, I_{\text{ori}}) \quad (\text{S36})$$

Subsequently, we calculate the LPIPS score between the reference image $I_{\text{ref}}^{\text{cont}}$ and the erased image I_{erase} :

$$L_{\text{erase}}^{\text{cont}} = \text{LPIPS}(I_{\text{ref}}^{\text{cont}}, I_{\text{erase}}) \quad (\text{S37})$$

To better measure the additional content degradation introduced during the erasure process, we calculate the difference:

$$C_{\text{content}} = L_{\text{erase}}^{\text{cont}} - L_{\text{base}}^{\text{cont}} \quad (\text{S38})$$

This difference value measures the additional perceptual difference potentially caused by content loss from removing the common style. When style erasure fails (typically preserving all content), the change between I_{ori} and I_{erase} is small. For the same reference system, the LPIPS scores should be close, so C_{content} should be close to 0. When the style erasure is successful and the content is well-preserved, I_{erase} and $I_{\text{ref}}^{\text{cont}}$ are closer, and C_{content} should be significantly less than 0. When the content is severely damaged, even with the reduction caused by style erasure (if only the style

Table S6. Quantitative results for CLIP Score. Our method obtains the best scores on both erasure completeness and content preservation, demonstrating that the AEC module removes style while providing the most comprehensive protection of content.

Category	ori	k	v	q	without	ours
Style	30.718	29.205	29.041	29.380	29.960	28.643
	30.810	28.683	28.492	29.079	29.699	28.152
	32.300	29.460	29.195	29.679	30.484	28.531
	31.939	29.736	29.588	29.865	30.631	28.948
	32.415	30.542	30.227	30.621	31.201	29.616
Content	25.510	26.692	27.068	26.831	27.039	27.604
	25.485	25.610	25.983	25.549	26.161	26.661
	25.020	26.119	26.516	25.520	26.314	26.744
	24.480	25.412	25.978	25.098	25.765	26.506
	26.420	28.210	29.015	28.105	28.187	28.665

Table S7. Quantitative results for LPIPS.

metric	ori	k	v	q	without	ours
$L(\text{ori}, \text{ref})$	–	0.572	0.603	0.535	0.531	0.610
	0.402	0.631	0.649	0.592	0.591	0.664
L_{style}	0.561	0.749	0.775	0.711	0.705	0.782
	0.486	0.686	0.725	0.663	0.640	0.737
L_{content}	0.772	0.713	0.757	0.709	0.752	0.716
	0.831	0.804	0.817	0.819	0.831	0.788

is erased and the content is well-preserved, C_{content} should be significantly less than 0), but due to severe content damage, C_{content} should be greater than 0. By weakening the influence of this style change, we make the remaining distance increment more sensitive to content degradation, thus making the metric more inclined to reflect the additional content degradation introduced during the erasure process. To make the metric more stable and robust, we use multiple reference styles to average the baseline. To validate this metric more intuitively, we provide an example in Figure S11.

B. Experimental Results

We present experimental results for six baselines (SPEED[23], ESD-x[11], ESD-u[11], FMN[50], MACE[27], SELECT[53]) and two artist styles, as shown in Figures S12, S13, S14, S15.

B.1. Ablation Study

B.1.1. Adaptive Erasure Controller

We present ablation results in Figure S16, Table S6, S7.

B.1.2. Attention Decoupling Editing

We present ablation results in Figure S17. The “Without Q strength” variant removes artistic style to some extent, but causes substantial damage to content and structure; objects, layout, and composition undergo pronounced

changes, whereas our method removes style while maximally retaining the original content arrangement. The “QKV-Before” and “QKV-Mixed” variants, although preserving part of the content structure, suffer from content drift in some cases. This shows that undifferentiated suppression of QKV not only fails to disentangle style and content, but also harms content information. Deterministic evaluation with LPIPS indicates that “QKV -before” yields better scores on style erasure C_{style} , yet is inferior on content preservation C_{content} . Moreover, comparing “QKV -before” with “without Q strength” reveals that “QKV -before” merely lacks the content-preserving operation of Q; while it improves style erasure, it incurs greater content damage. We know that Q also contains stylistic features, but it primarily carries content information. Our results across diverse examples consistently show that our QKV decoupling editing is superior: it achieves style removal while preserving the intended content. These findings support our design choice: the key to accurate heterogeneous editing is to compute attention with content enhancement guiding structural retention (via Q) and to use KV for style suppression, thereby maximizing style removal while preserving content.

B.2. Hyperparameter Sensitivity

B.2.1. Feature Extraction Diffusion Interval

We conduct an extended study on the diffusion-step interval used for feature extraction. The entire diffusion process is partitioned into ten contiguous, non-overlapping intervals of 100 steps each, and experiments are performed within every interval; representative results are presented in Figures S18 and S19. The optimal feature-extraction interval is 100–400 steps, where content structure is already stable while style has not yet fully formed, yielding the highest separability and the best style–content decoupling. In the later diffusion phase (500–899), substantial chaotic textures and other artifacts emerge; at this stage the style subspace tends to align with unstable texture directions. When features are extracted at the final synthesis phase (900–999), the style subspace captures globally stable textures and color patterns, which makes decoupling style from content difficult.



Figure S12. Quantitative results for erasing "Van Gogh" and preserving "village". Some baseline solutions dismantled the original village elements, generating chaotic, collage-like scenes. Others failed to achieve complete stylistic erasure—despite removing certain components, the background retained "Van Gogh" brushstrokes and textures. These approaches primarily replaced styles (with oil painting or cartoon styles) rather than truly erasing them. Our solution precisely targets stylistic features and achieves accurate style erasure (rotating brushstrokes and unique color patterns). Our processed images retain a high degree of fidelity in village layout, house structures, and roadways, demonstrating the superiority of our algorithm in decoupling style from content and its efficiency in precise style removal.



Figure S13. Quantitative results for erasing "Van Gogh" and preserving "apple". In this case, nearly all solutions cleanly erased the artistic style. However, most baseline approaches tended toward destructive image reconstruction—placing "apple" within picture frames or disrupting its form to generate chaotic color blocks and structures. This resulted in fragmented, discolored, or morphologically distorted "apple" representations that failed to preserve fundamental content integrity. Additionally, some samples retained partially erased brushstroke textures. Our solution demonstrates precise style removal capabilities, successfully stripping away the original image's strong artistic elements (rotation, brushstrokes, etc.) while maximally preserving the "apple" form, lighting relationships, and background composition. This results in a clean, de-stylized image, indicating our algorithm accurately identifies stylistic features for precise removal without compromising content authenticity.



Figure S14. Quantitative results for erasing “Van Gogh” and preserving “tulip”. After processing with our solution, the tulips appear full and natural in form, with clean petal edges and smooth color transitions. This transforms a stylized, high-contrast piece into a clean, harmonious image while preserving the original structure to the greatest extent possible.

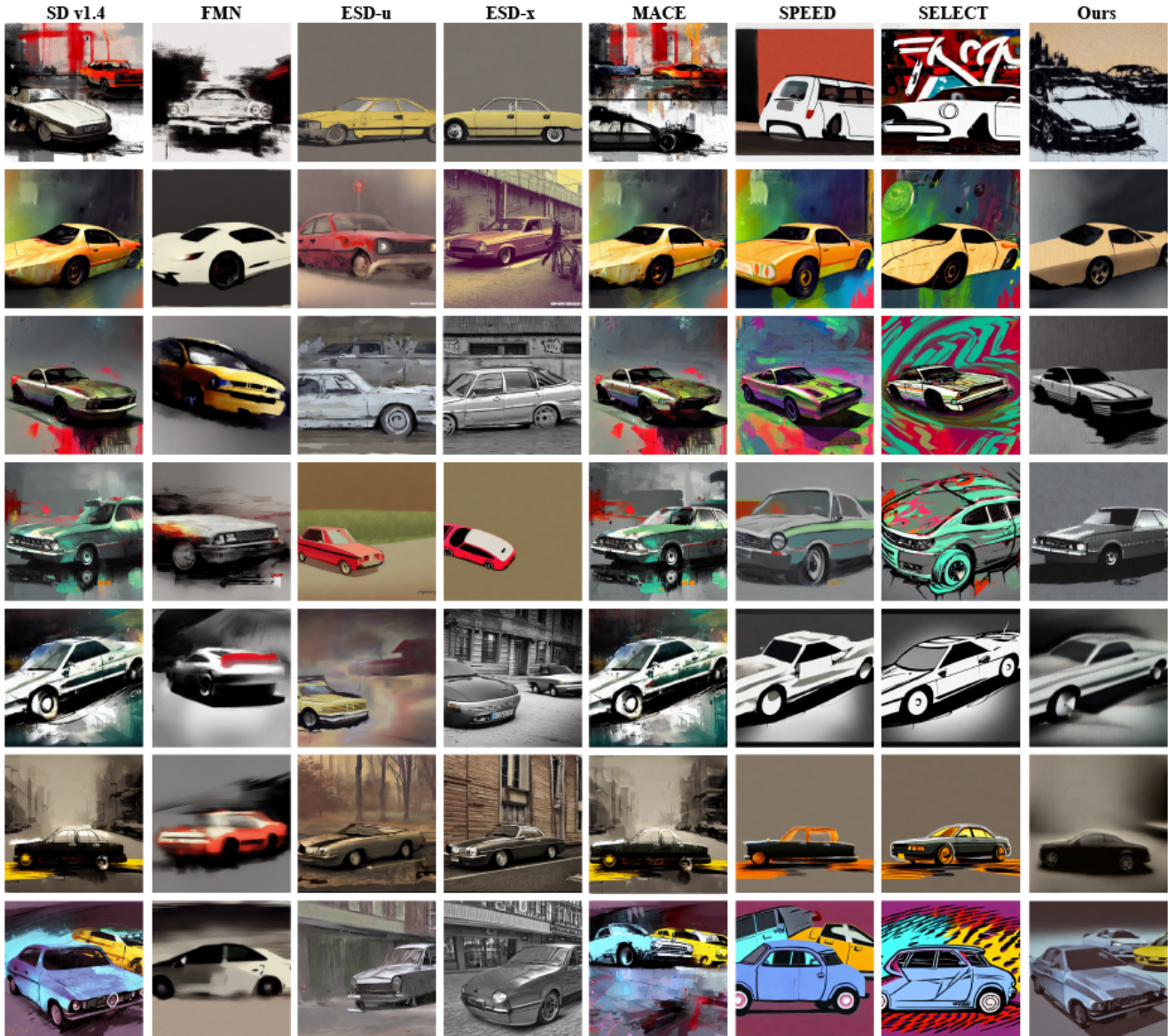


Figure S15. Quantitative results for erasing “Adrian Ghenie” and preserving “car”. The characteristics of this artistic style are dynamic and blurred brushstrokes, with explosive bright colors interspersed in dim tones. The erasure process requires the removal of not only the brushstrokes but also the unique color patterns. Faced with this highly challenging artistic style, it can be observed from the results that half of the baseline methods failed in the erasure, still retaining tones and brushstrokes similar to the original artistic style, while other baselines generated images with distorted shapes and blurred details. Our method accurately locates and removes the dragging brushstrokes and intense color patterns. In the images processed by our method, the car body structure is clear, and the intense colors are eliminated. This demonstrates that for such styles with high erasure difficulty, our algorithm can still perform efficient style recognition by constructing suitable contrastive sample sets, enabling the model to deeply understand complex, non-local style features such as “dynamic blur” and “intense colors,” and achieve precise style erasure while preserving content integrity.

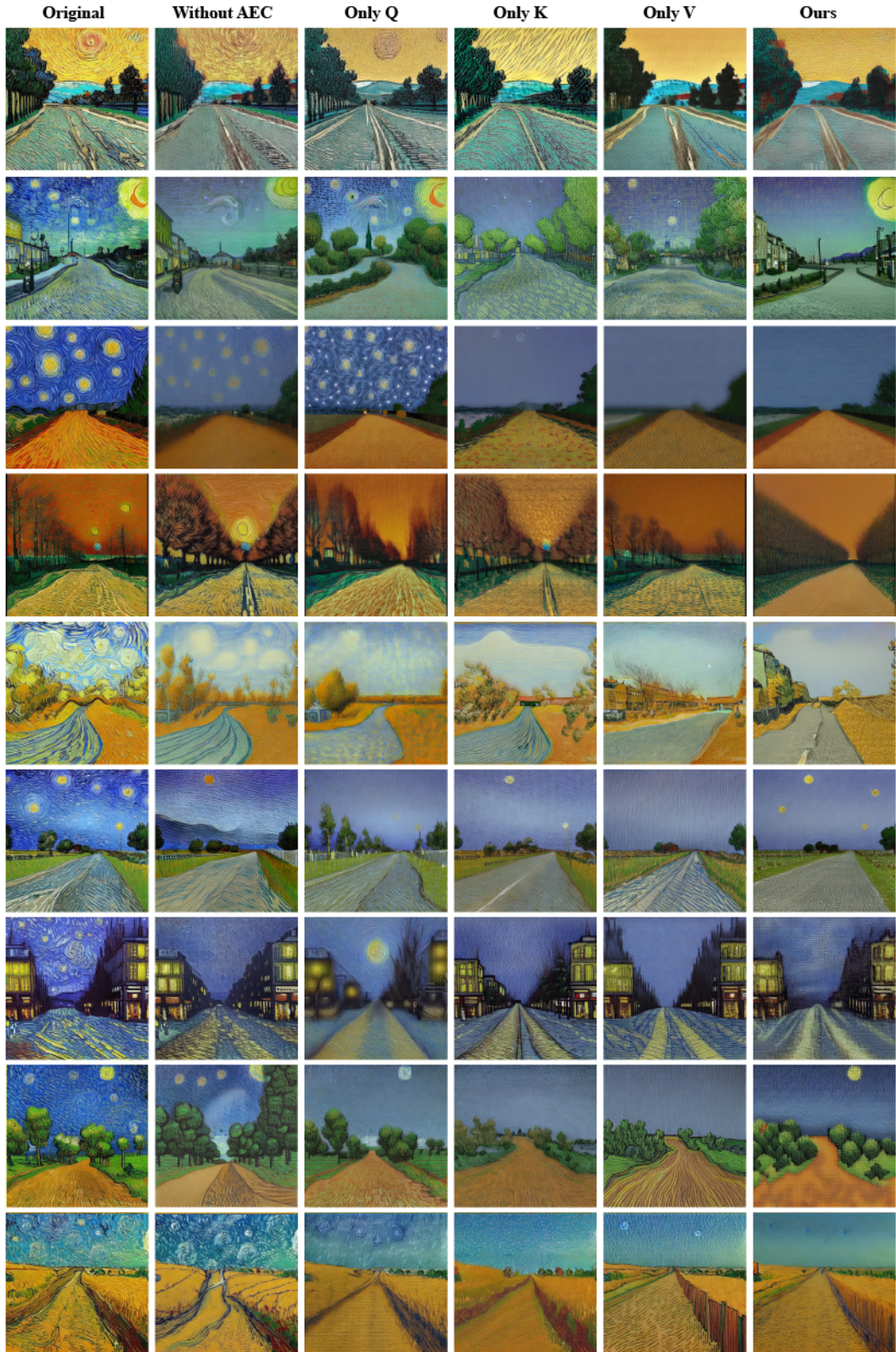


Figure S16. Ablation study of the Adaptive Erasure Controller. We compare our full model (Ours) with the following variants: (1) Without AEC: erasure with a uniform strength; (2) Only Q: style scoring using Q only; (3) Only K: style scoring using K only; (4) Only V: style scoring using V only.



Figure S17. Ablation study of Attention Decoupling Editing. We compare our module with three variants: (1) Without Q strength: remove content enhancement and apply KV-only style suppression; (2) QKV-Before: perform heterogeneous editing on QKV before attention fusion; (3) QKV-Mixed: perform heterogeneous editing on QKV after attention fusion.

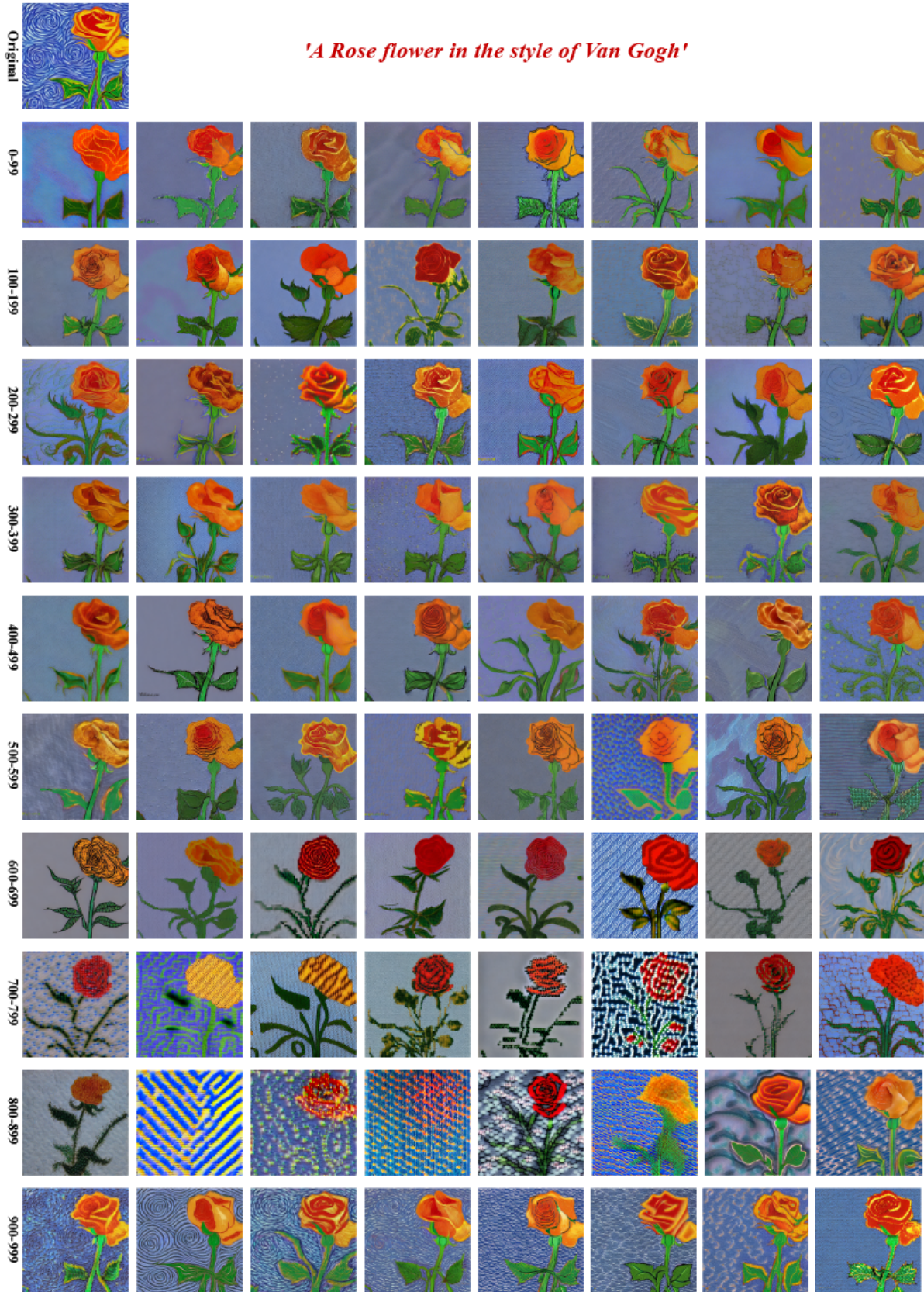


Figure S18. Hyperparameter sensitivity test of the feature-extraction interval on style erasure for “a rose in the style of Van Gogh.” Each row shows erasure results obtained by extracting style features within a 100-step diffusion interval.

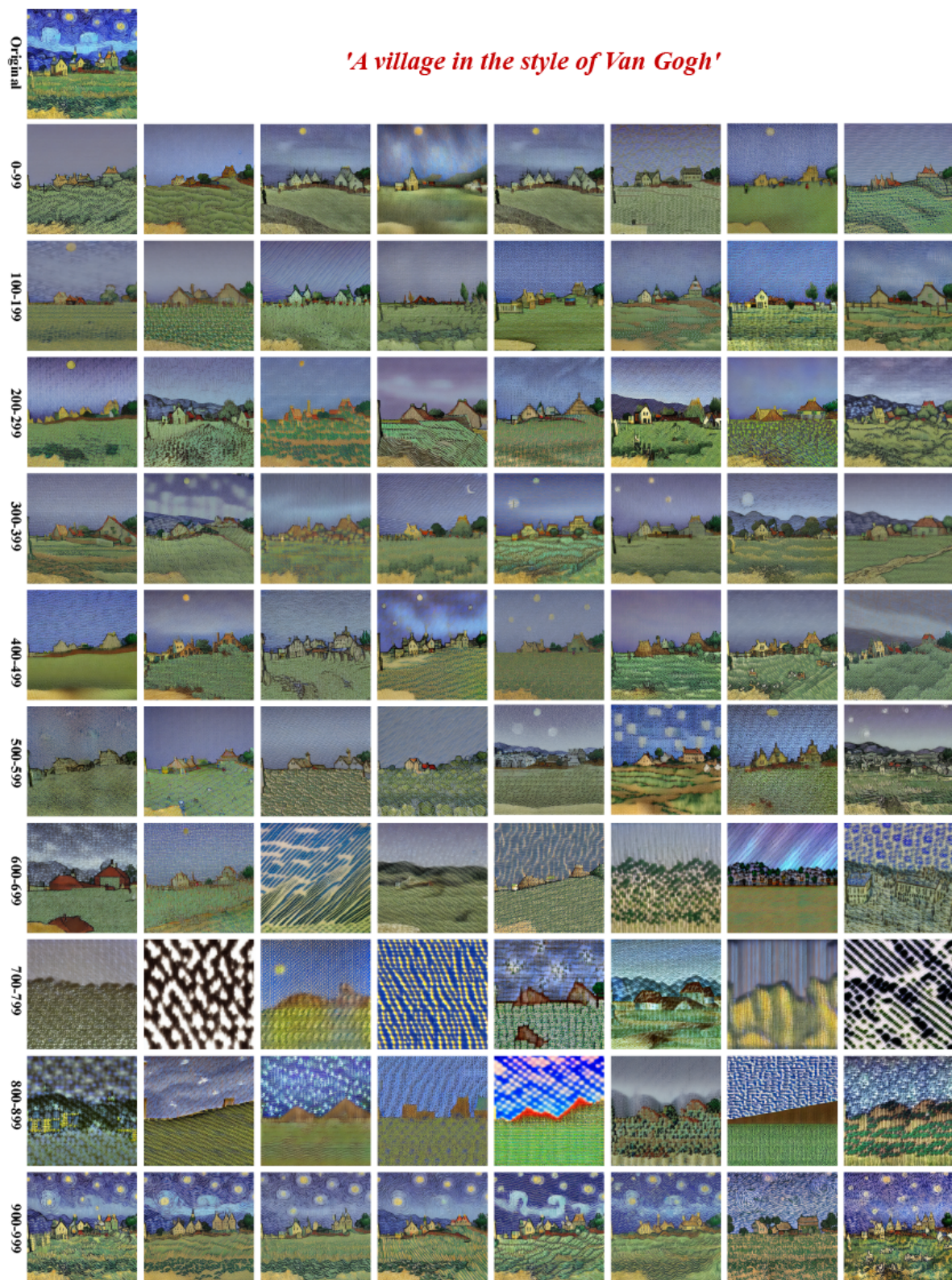


Figure S19. Hyperparameter sensitivity test of the feature-extraction interval on style erasure for “a village in the style of Van Gogh.”